Electronic Supplementary Material (ESI) for Journal of Materials Chemistry A.
This journal is © The Royal Society of Chemistry 2018

Supplementary Information

Quasi-parallel Arrays of 2D-on-2D Structure for Electrochemical Supercapacitors

Xiaolong Guo[a,b], Tian Wang[a], Tian Xu Zheng[a], Chaohe Xu[b], Jintao Zhang[c],

Yu Xin Zhang[a,], Xiao Ying Liu[d,]*, Fan Dong[d]*

[a]State Key Laboratory of Mechanical Transmissions, College of Materials Science and Engineering, Chongqing University, Chongqing 400044, P.R. China
E-mail addresses: zhangyuxin@cqu.edu.cn

[b]College of Aerospace Engineering, and State Key Laboratory of Mechanical Transmissions, Chongqing University, No.174 Shazhengjie Road, Chongqing 400044, P.R. China

[c]Key Laboratory of Colloid and Interface Chemistry, Ministry of Education, School of Chemistry and Chemical Engineering, Shandong University, Jinan 250100, P.R. China

[d] Engineering Research Center for Waste Oil Recovery Technology and Equipment of Ministry of Education, College of Environment and Resources, Chongqing Technology and Business University, Chongqing, 400067, China
E-mail addresses: lxy_ctbu@163.com

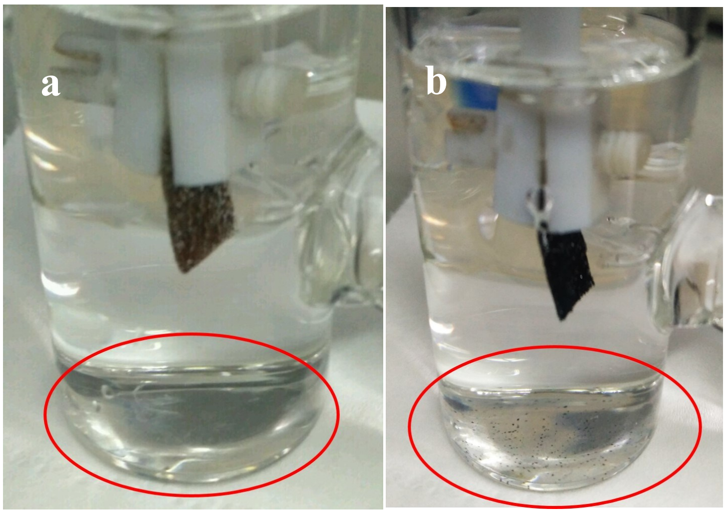

Fig. S1 After a continuous 1,000th charge-discharge, the comparison of fall out amount of active materials: (a) NiMn oxide@MnO_2 arrays; (b) $NiCo_2O_4$ nanowire arrays.

After a continuous process of charge-discharge, the $NiCo_2O_4$ nanowire arrays occurred drop off from current collectors. The black powder had dropped onto the bottom of electrolytic cell. On the contrary, the NiMn oxide@MnO_2 arrays had hardly any fall out.

Movie S1 The experiment of external force: the electrodes are scraped by blade. (a) NiMn oxide@MnO_2 arrays; (b) $NiCo_2O_4$ nanowire arrays.

In the tests (Movie S1), lots of black powder from the $NiCo_2O_4$ nanowire arrays gradually fall on the filter paper. In the same test, the NiMn oxide@MnO_2 arrays have no obviously dropped down. Therefore, comparing with nanowire arrays, the quasi-parallel arrays with smaller aspect ratio has stronger structural connection with current collector.

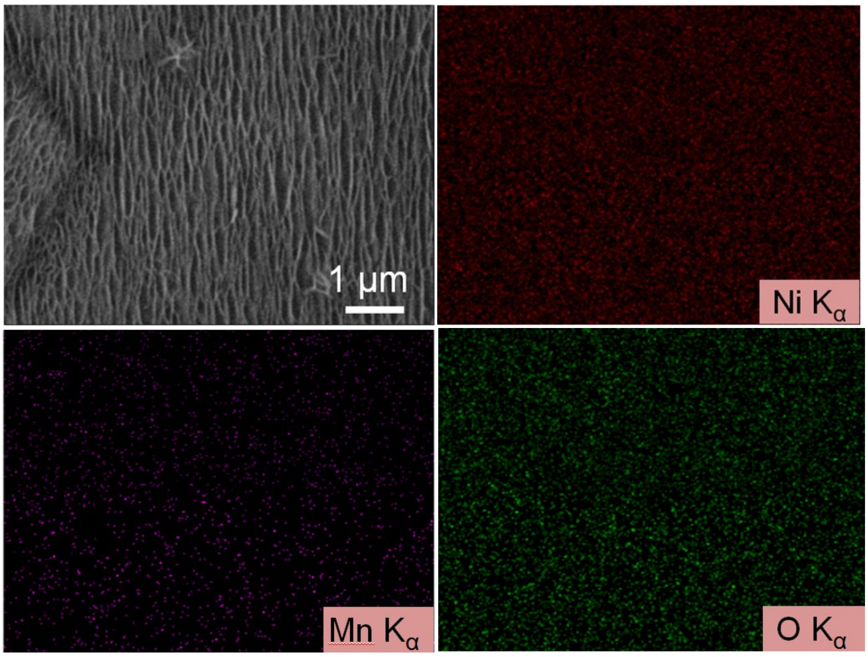

Fig. S2 EDS mapping of NiMn oxide on Ni foam.

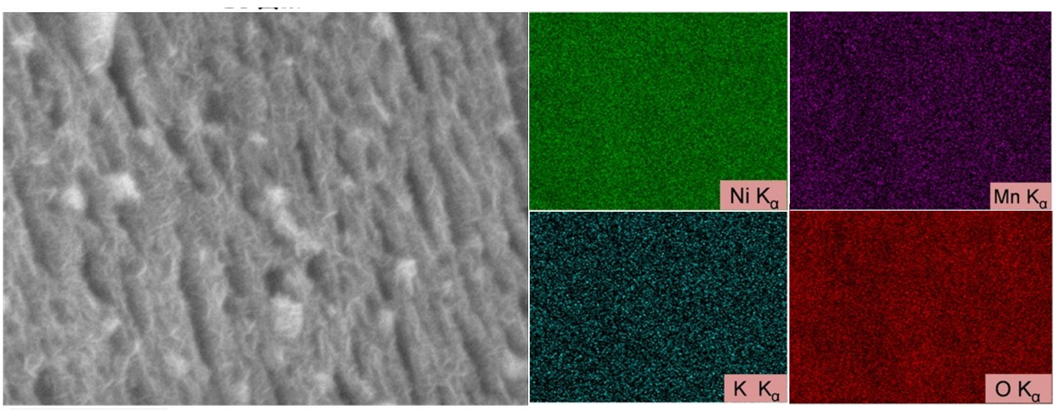

Fig. S3 EDS mapping of K, Ni, Mn, and O elements on individual NiMn oxide@MnO_2 arrays.

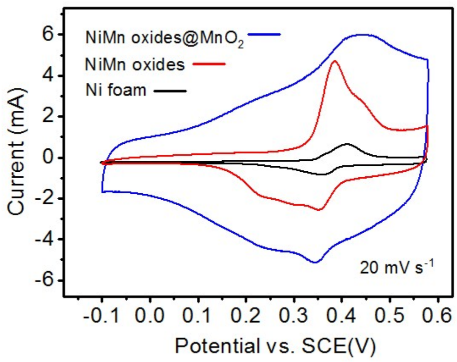

Fig. S4 Cyclic voltammograms of pure Ni foam, NiMn oxide and NiMn oxide@MnO_2 at a scan rate of 20 mV s $^{-1}$.

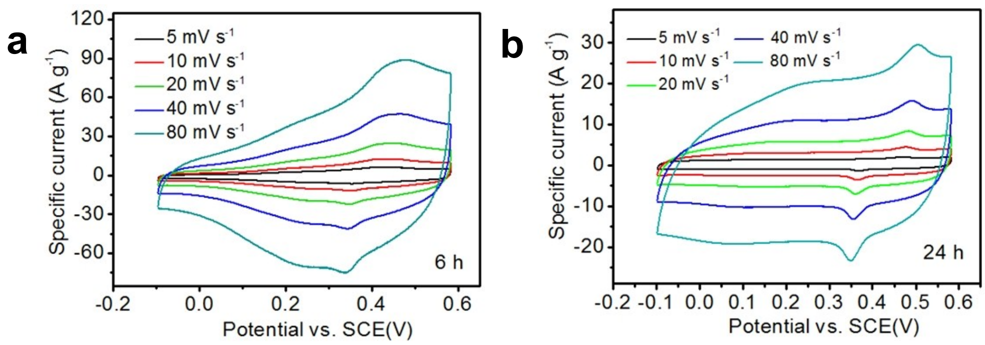

Fig. S5 Cyclic voltammograms (specific current versus potential) for two NiMn oxide@MnO_2 electrodes (hydrothermal time: 6 h (a) and 24 h (b)) at five different scan rates between 5 and 80 mV s^{-1}.

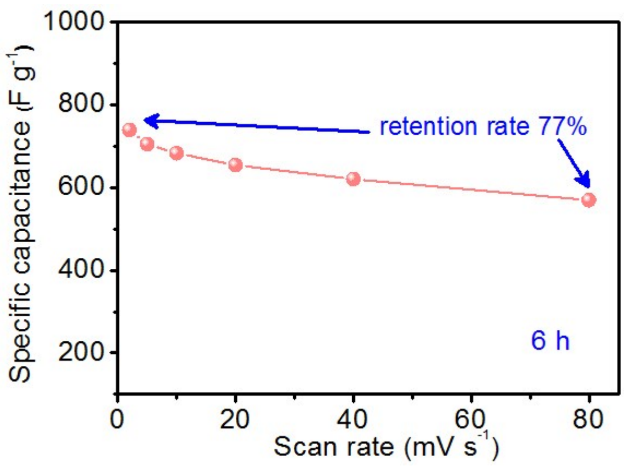

Fig. S6 Specific capacitance of the NiMn oxide@MnO_2 (6 h) electrode versus scan rate. Consisting with CC tests, the NiMn oxide@MnO_2 (6 h) electrode still shows high rate capability.

Table S1 Comparison of the supercapacitor performances of the reported MnO_2 shell-core arrays (1D/2D structure) based electrodes in the three-electrode system with aqueous electrolytes.

Electrode materials	Specific capacitance	Rate capability	Cycle stability	Mass of MnO_2	Electrolyte solution	Ref.
NiMn oxide @MnO_2 quasi-parallel arrays	**801 F g^{-1} at 1 A g^{-1} 739 F g^{-1} at 2 mV s^{-1}**	**Retain 79% (629 F g^{-1} at 40 A g^{-1})**	**Retain98.7% (5,000 cycles)**	**0.25 mg cm^{-2}**	**LiOH (1 M)**	**This work**
Ti foil @ATO@MnO_2	216 F g^{-1} at 1 A g^{-1}	Retain 75% (162 F g^{-1} at 20 A g^{-1})	Retain 93.8% (5,000 cycles)	------	Na_2SO_4 (1 M)	Nano Res., 2015, 8, 990
Carbon fabrics $CuCo_2O_4$@MnO_2	327 F g^{-1} at 1.25 A g^{-1}	Retain 90% (296 F g^{-1} at 6.25 A g^{-1})	Retain 93% (2,000 cycles)	0.5 mg cm^{-2}	KOH (3 M)	ChemElectroChem, 2014, 1, 559
Cu grid@ CuO@MnO_2	343.9 F g^{-1} at 0.25 A g^{-1}	Retain 70.5% (242.5 F g^{-1} at 5 A g^{-1})	Retain 83% 12,000 cycles	------	Na_2SO_4 (1 M)	J. Mater. Chem. A, 2016, 4, 10786
Ni foam@ ZnO@MnO_2	423.5 F g^{-1}at 0.5 A g^{-1}	Retain 41% (175 F g^{-1} at 10 A g^{-1})	Retain 92% (3,000 cycles)	------	Na_2SO_4 (0.5 M)	Electrochimica Acta, 2015,152, 172-
Carbon cloth @H-TiO_2@MnO_2	449.6 F g^{-1} at 10 mV s^{-1}	Retain 54.6% (245 F g^{-1} at 200 mV s^{-1})	------	0.19-0.23 mg cm^{-2}	LiCl (5 M)	Adv. Mater., 2013, 25, 267
Stainless steel@ Co_3O_4@MnO_2	480 F g^{-1} at 2.67 A g^{-1}	Retain 56% (267 F g^{-1}at 29.8 A g^{-1})	Retain 97.3% (5000 cycles)	0.8 mg cm^{-2}	LiOH (1 M)	Adv. Mater., 2011, 23, 2076
Ti foil @TiN nanotubes@MnO_2	486 F g^{-1} at 2 mV s^{-1}	------	Retain 97% (1,000 cycles)	0.06 mg cm^{-2}	Na_2SO_4 (1 M)	Energ. Environ. Sci., 2011, 4, 3502
Stainless steel@ SnO_2@MnO_2 nanowires	637 F g^{-1} at 2 mV s^{-1}	Retain 55% (350 F g^{-1} at 100 mV s^{-1})	Retain 98.8% (2,000 cycles)	0.08 mg cm^{-2}	Na_2SO_4 (1 M)	ACS Nano, 2010, 4, 4247
Carbon microfibers@ Zn_2SnO_4@MnO_2	642.3 F g^{-1} at 1 A g^{-1}	Retain 64.4% (413.9 F g^{-1} at 40 A g^{-1}	Retain 98.8% (1,000 cycles)	------	Na_2SO_4 (1 M)	Nano Lett. 2011, 11, 1215
Ti6Al4V alloy@ TiC@C@MnO_2	645 F g^{-1} at 1 A g^{-1}	Retain 44.7% (288 F g^{-1}at 25 A g^{-1})	Retain 99% (5,000 cycles)	------	Na_2SO_4 (1 M)	Small, 2015, 11, 1847
Carbon fabric@ carbon nanoparticles @MnO_2 nanorods	800 F g^{-1} at 5 mV s^{-1}	Retain 50% (400 F g^{-1} at 100 mV s^{-1})	------	0.201 mg cm^{-2}	Na_2SO_4 (0.1 M)	ACS Nano, 2011, 6, 656

Electrode materials	Specific capacitance	Rate capability	Cycle stability	Mass of MnO_2	Electrolyte solution	Ref.
NiMn oxide@MnO_2 quasi-parallel arrays	**801 F g^{-1} at 1 A g^{-1} 739 F g^{-1} at 2 mV s^{-1}**	**Retain 79% (629 F g^{-1}, 40 A g^{-1})**	**Retain98.7% (5,000 cycles)**	**0.25 mg cm^{-2}**	**LiOH (1 M)**	**This work**
Tubular Ag/MnO_2	170 F g^{-1} at 1 mV s^{-1}	Retain 24% (40 F g^{-1}, 100 mV s^{-1})	Retain 80% (1,000 cycles)	-------	Na_2SO_4 （1 M）	J. Phys. Chem. C 2014, 118, 6604
Ag nanoparticles @MnO_2 hybrid nanowires	293 F g^{-1} at 10 mV s^{-1}	Retain 62% (183 F g^{-1}, 100 mV s^{-1})	Retain 92.5% (5,000 cycles)	-------	Na_2SO_4 （1 M）	J. Mater. Chem. A, 2015, 3, 1216
MnO_2 @Ag nanowire	423.5 F g^{-1} at 6 A g^{-1}	-------	Retain 157% (7,000 cycles)	0.3 mg cm^{-2}	Na_2SO_4 （0.5 M）	Chem. Commun., 2016, 52, 7998
Ti@Co_3O_4@Pt@ MnO_2 arrays	539 F g^{-1} at 1 A g^{-1}	Retain 55.3% (298.1 F g^{-1}, 40 A g^{-1})	Retain 105.6% (5,000 cycles)	0.1 mg cm^{-2}	Na_2SO_4 (1 M)	Sci. Rep., 2013, 3, 2978
Carbon fabric@WO_{3-x}@Au@MnO_2 arrays	588 F g^{-1} at 10 mV s^{-1}	Retain 41% (240 F g^{-1}, 100 mV s^{-1})	-------	0.05 mg cm^{-2}	Na_2SO_4 （0.1 M）	Adv. Mater. 2012, 24, 938
PAN@AuPd@ MnO_2 nanopillar arrays	603 F g^{-1} at 5 mV s^{-1}	Retain 58% (350 F g^{-1}, 100 mV s^{-1})	Retain 93% (5,000 cycles)	0.01 mg cm^{-2}	Na_2SO_4 (1 M)	Adv. Mater., 2013, 25, 3302
Nanoporous gold @Au-doped MnO_2 films	626 F g^{-1} at 5 mV s^{-1}	Retain 80% (500 F g^{-1}, 100 mV s^{-1})	Retain 93% (15,000cycles	0.025 mg cm^{-2}	Li_2SO_4 (2 M)	Angew. Chem. Int. Edit., 2013, 125, 1708
Copper foil @CuO@AuPd nanoparicles @MnO_2 arrays	876 F g^{-1}at 1 mA cm^{-2}	Retain 46% (400 F g^{-1},10 mA cm^{-2})	-------	0.04 mg cm^{-2}	KOH (1 M)	Adv. Mater., 2014, 26, 4279
Carbon fabric		Retain 31%	Retain 103%	[illegible]	Na_2SO_4	Nano Lett.,

@N-CNTs@Au nanoparticles@ MnO_2 arrays	1091 F g^{-1} at 5 mV s^{-1}	(341 F g^{-1}, 500 mV^{-1})	(5,000 cycles)		(1 M)	2016, 16, 40
Nanoporous gold@MnO_2 film	1,145 F g^{-1} at 50 mV s^{-1} (601 F g^{-1} at 0.5 A g^{-1})	Retain 74% (850 F g^{-1}, 50 mV s^{-1})	Retain 85% (1,000 cycles)	-------	Li_2SO_4 (2 M)	Nat. Nanotech., 2011, 6, 232

Table S2 Comparison of the supercapacitor performances of the reported MnO_2@noble metal electrodes in the three-electrode system with aqueous electrolytes.

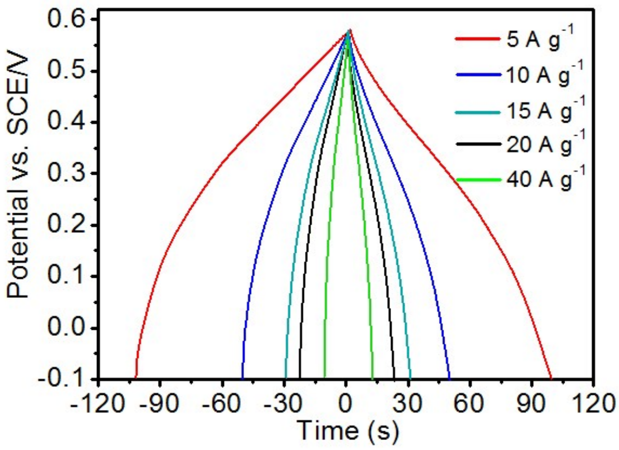

Fig. S7 Charge-discharge curves of NiMn oxide@MnO_2 (6 h) at the five different specific currents.

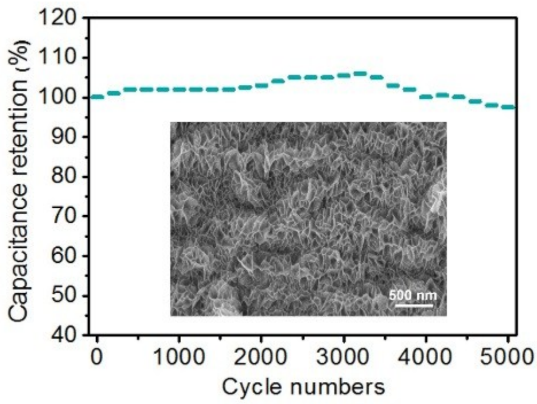

Fig. S8 Cycle performance of NiMn oxide@MnO_2 (24 h) at 7.5 A g^{-1}. The inset is SEM image of NiMn oxide @MnO_2 electrode (24 h) after cycling.

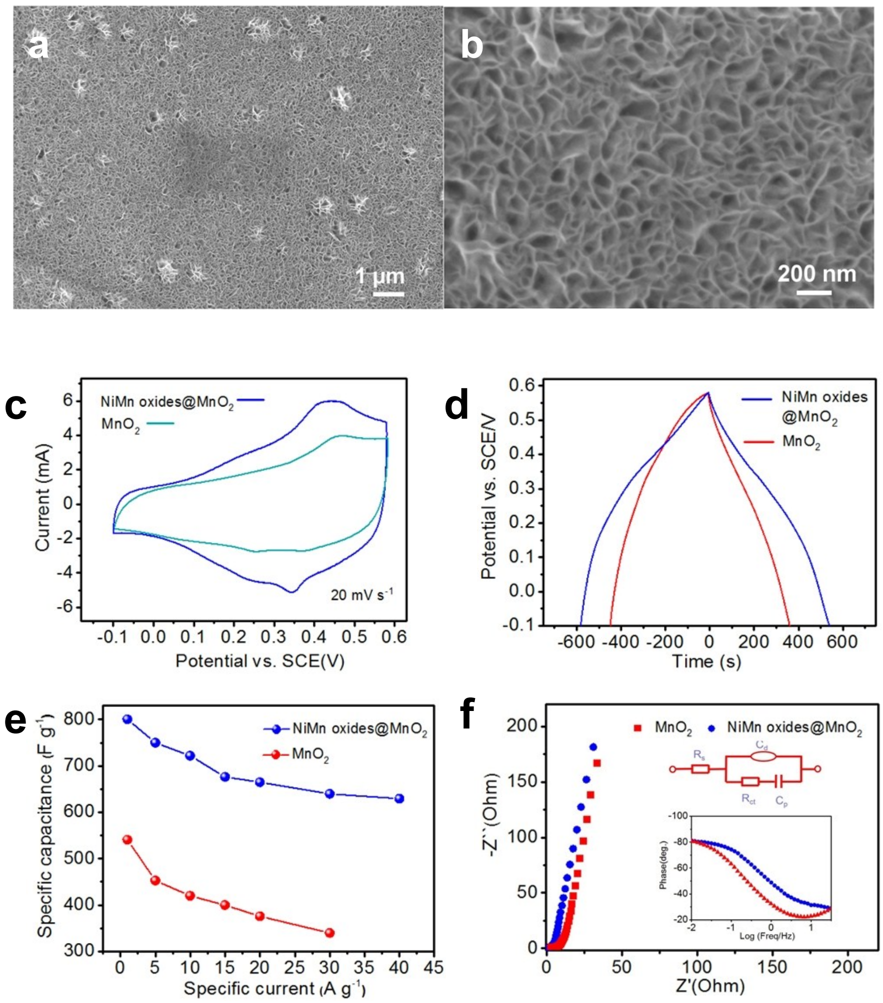

Fig. S9 (a) and (b) SEM images of the MnO_2 nanosheets on Ni foam. The mass loading of MnO_2 is 0.25-0.3 mg cm^{-2}. Comparative electrochemical properties of NiMn oxide and NiMn oxide@MnO_2: (c) cyclic voltammograms at a scan rate of 20 mV s^{-1}; (d) Charge-discharge curves at 1 A g^{-1}; (e) specific capacitance (C_s) versus discharge currents; (f) initial electrochemical impedance spectrums, the insets show phase angle versus frequency and equivalent circuit model, respectively.

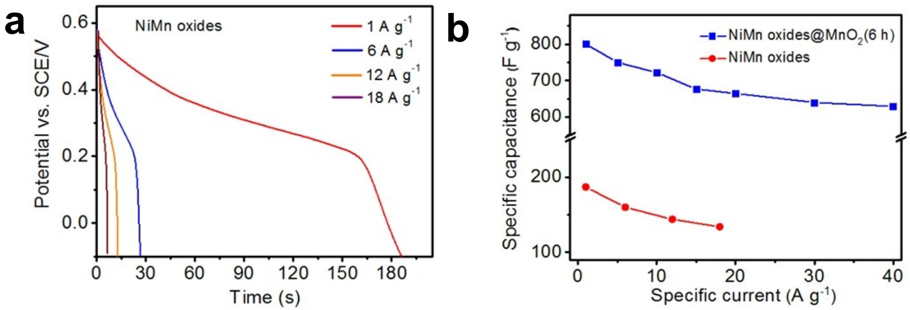

Fig. S10 (a) Discharge curves at different specific currents for NiMn oxide; (b) Comparative specific capacitance of NiMn oxide and NiMn oxide@MnO_2 at different specific currents.

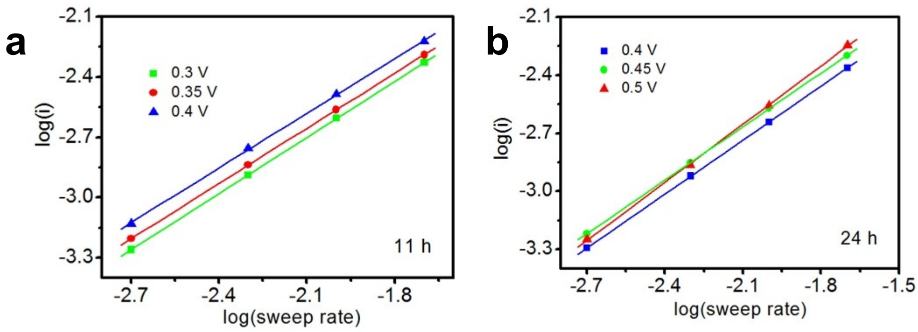

Fig. S11 Power law dependence of anodic peak currents on various scan rates for 11 h and 24 h electrodes.

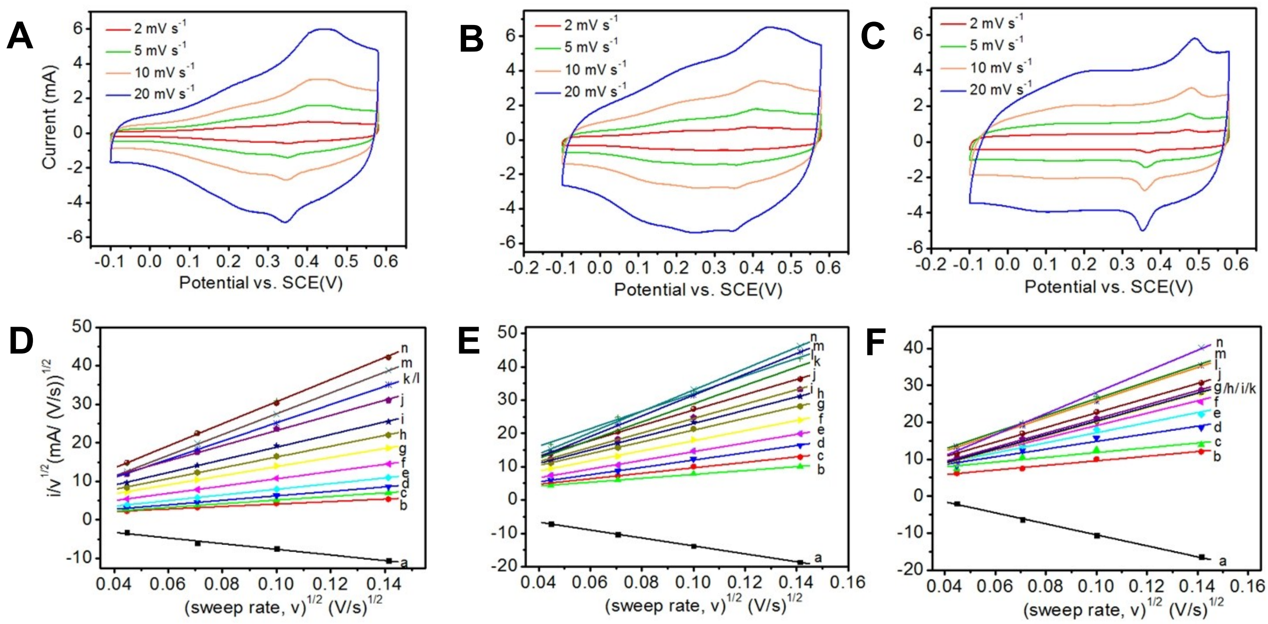

Fig. S12 (A-C) Cyclic voltammograms (current versus potential) for three NiMn oxide@MnO_2 (hydrothermal time: 6 h (A), 11 h (B) 24 h and (C)) electrodes at four different scan rates between 2 and 20 mV s^{-1}. (D-F) The sweep rate dependence of the current at various potential for NiMn oxide@MnO_2 (6 h (D), 11 h (E) and 24 h (F)) electrodes according to eq (3) : (a) -0.1, (b) -0.05, (c) 0, (d) 0.05, (e) 0.1, (f) 0.15, (g) 0.2, (h) 0.25, (i) 0.3, (j) 0.35, (k) 0.4, (l) 0.45, (m) 0.5 and (n) 0.55 V. Scan rates were varied from 2 to 20 mV s^{-1} in the anodic region.

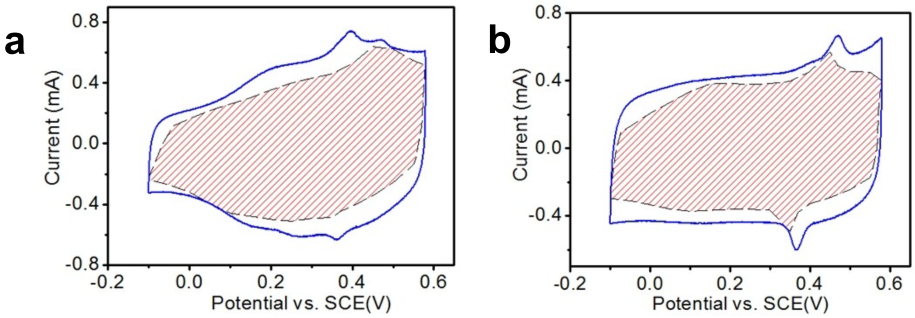

Fig. S13 Voltammetric responses for NiMn oxide@MnO_2 electrodes at a scan rate of 2 mV s^{-1}: (a) 11 h and (b) 24 h. The surface capacitive contribution to the total current is shown by the red shaded region.

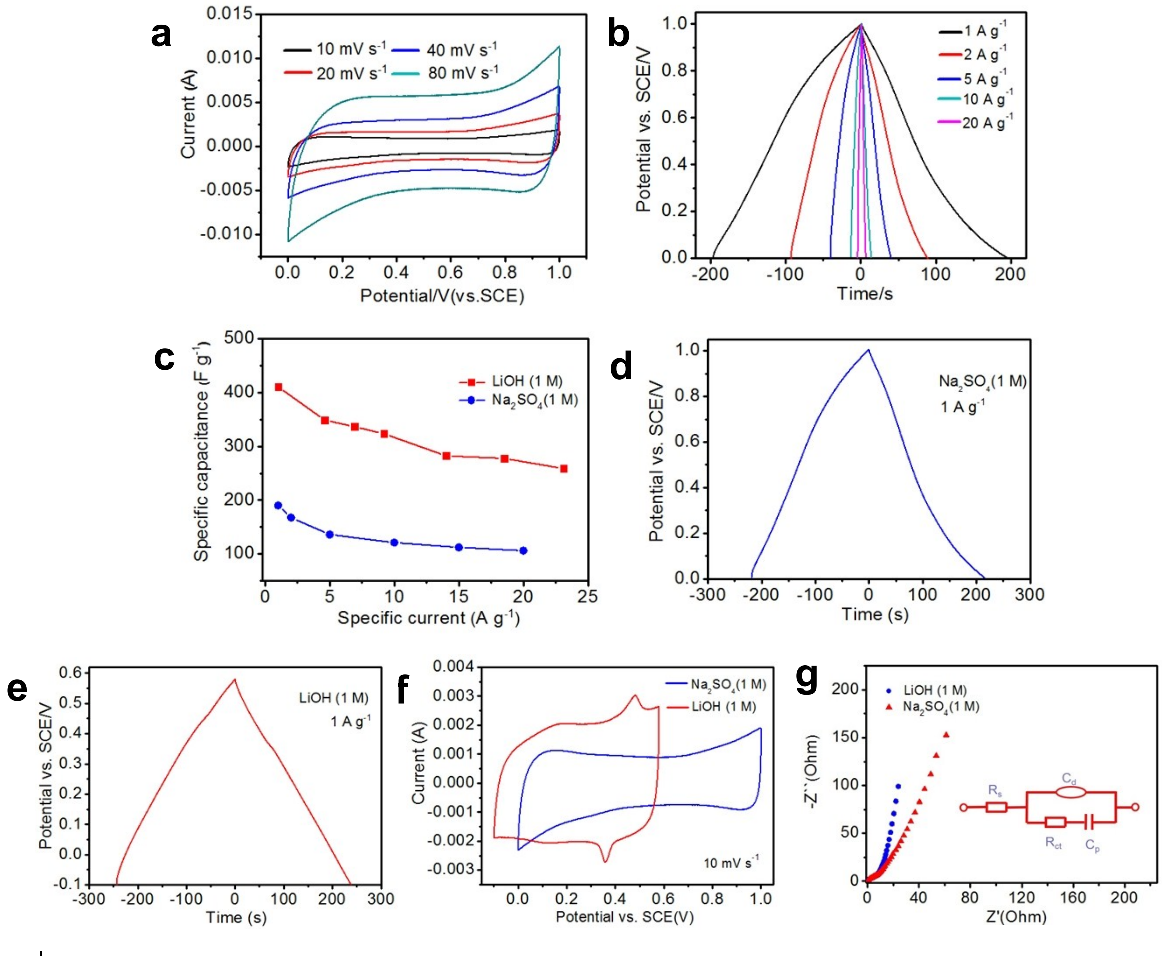

Fig. S14 (a) Cyclic voltammograms (current versus potential) for NiMn oxide@MnO_2 (hydrothermal time: 24 h) electrode in Na_2SO_4 (1 M) solution at four different scan rates between

10 and 80 mV s^{-1}. (b) Charge/discharge (potential versus time) curves at various specific currents. Comparative electrochemical behaviors for NiMn oxide@MnO_2 electrodes (24 h) at Na_2SO_4 (1 M) and LiOH (1 M) aqueous electrolytes: (c) Specific capacitance at various specific currents; (d, e) Galvanostatic charge/discharge curves; (f) Cyclic voltammetry curves; (g) Electrochemical impedance spectroscopy, the inset is equivalent circuit model.

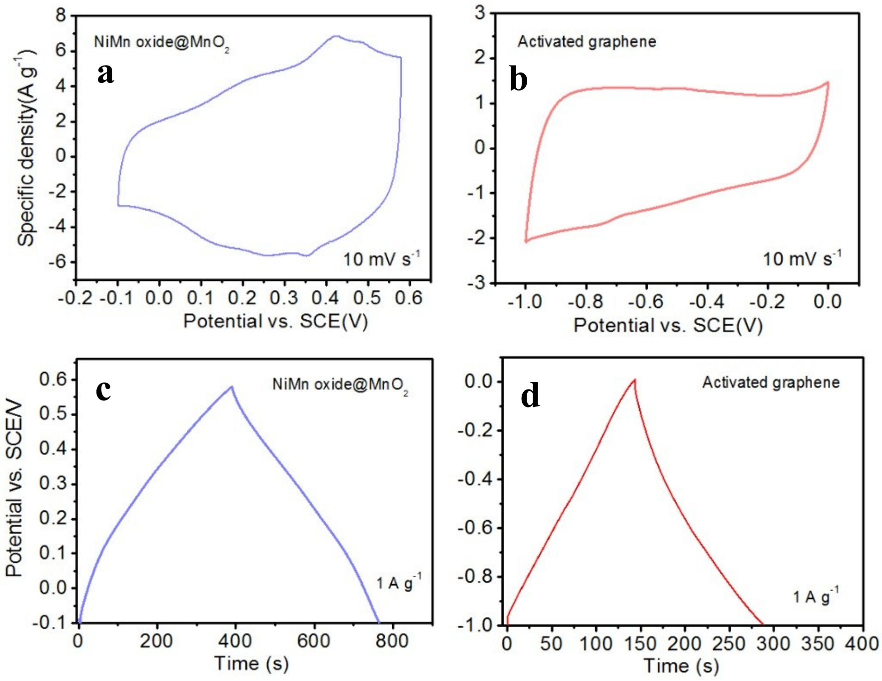

Fig. S15 Cyclic voltammograms (specific current versus potential) of (a) the NiMn oxide@MnO_2 (11 h) positive electrode and (b) the activated graphene negative electrode; Charge-discharge curves of (c) the NiMn oxide@MnO_2 positive electrode (11 h) and (d) the activated graphene negative electrode at 1 A g^{-1}.

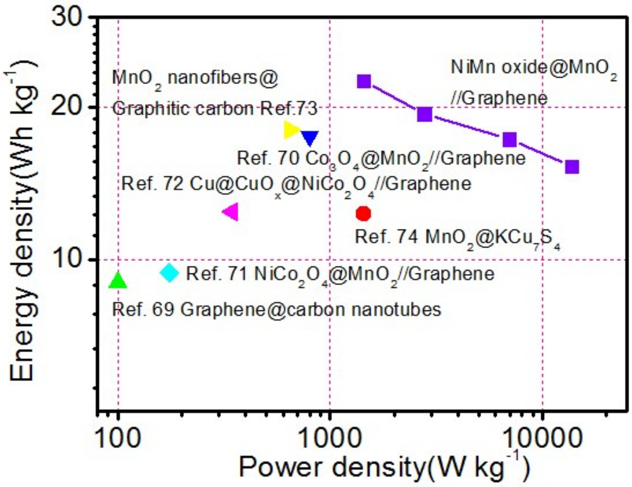

Fig. S16 Power and energy densities of the various asymmetric supercapacitors.